

Boundaries, Cusps and Caustics in the Multimagnon Continua of 1D Quantum Spin Systems.

T. Barnes

Physics Division, Oak Ridge National Laboratory,

Oak Ridge, TN 37831-6373

and

Department of Physics and Astronomy, University of Tennessee,

Knoxville, TN 37996-1501

October 24, 2018

Abstract

The multimagnon continua of 1D quantum spin systems possess several interesting singular features that may soon be accessible experimentally through inelastic neutron scattering. These include cusps and composition discontinuities in the boundary envelopes of two-magnon continuum states and discontinuities in the density of states, “caustics”, on and within the continuum, which will appear as discontinuities in scattering intensity. In this note we discuss the general origins of these continuum features, and illustrate our results using the alternating Heisenberg antiferromagnetic chain and two-leg ladder as examples.

1 Two-magnon states

1.1 Introduction and definitions

Recently the subject of two-magnon excitations of quasi-1D quantum spin systems has attracted considerable interest. Theorists have long predicted that some of these systems will possess bound states [1], and there are now experimental indications of such bound states in the alternating chain material copper nitrate [2] and in the spin ladder $(\text{Ca,La})_{14}\text{Cu}_{24}\text{O}_{41}$ [3, 4].

In addition to the bound modes there is a continuum of two-magnon states, which has been reported in inelastic neutron scattering from polycrystalline $\text{Sr}_{0.73}\text{CuO}_2$ [5] (assuming an alternating chain model) and copper nitrate single crystals [2]. Although this continuum has been considered a rather uninteresting feature in comparison with the bound states, it actually possesses an interesting and rather complicated internal structure [6, 7]. With high resolution inelastic neutron scattering experiments it should be possible to study these features of the two-magnon continuum in parallel with studies of the bound modes. To facilitate these experiments, here we discuss the nature of these interesting features of the continuum and show how they can be understood simply in terms of aspects of the one-magnon modes.

The two-magnon continuum states in a gapped 1D antiferromagnet are simply composed of two one-magnon excitations, since the interaction region is a zero matrix element for these unlocalized states. The energy of a two-magnon state composed of magnons with k_1 and k_2 is therefore given by

$$\omega_2(k = k_1 + k_2) = \omega(k_1) + \omega(k_2) \quad (1)$$

with the usual crystal momentum constraints on k_1, k_2 and k ,

$$k = k_1 + k_2 \text{ mod}(2\pi) . \quad (2)$$

Thus the allowed states in the two-magnon continuum are given by the simple vector addition of Fig.1.

For a fixed two-magnon k we can independently vary k_1 , keeping $k_2 = k - k_1$. This gives a range of allowed two-magnon energies for given k . Carrying out this “scan” in k_1 at each k gives the full set of states in the two-magnon continuum. Interesting physics questions regarding this continuum include the determination of the upper- and lower- limit boundary curves of this allowed region, and the composition of the two-magnon states along and within these boundaries.

All this information is implicit in the one-magnon dispersion relation $\omega(k)$. In the following discussion unless otherwise specified we will assume that $\omega(k)$ is an even, periodic function of k with period 2π , monotonically increasing inside the range $k = [0, \pi]$, with a single inflection point at k_0 . We also assume that $\omega(k)$ departs from its $k = 0$ minimum and $k = \pm\pi$ maximum values quadratically in k , and that the inflection point lies within $|k| = [0, \pi/2]$. (This $\omega(k)$ is abstracted from the simple alternating chain result, shown in Fig.1. Our discussion can easily be extended to more general cases.)

1.2 Lower continuum boundary

First we consider the lower boundary of the two-magnon continuum, which we call $\Omega_2^-(k)$. The $k = 0$ two-magnon mode clearly has a lower boundary at $\omega_2(0) = 2\omega(0)$, since this satisfies the momentum

constraint $k = k_1 + k_2 \text{ mod}(2\pi)$ and is the global minimum of free two-magnon energies. For other k values we wish to solve

$$\Omega_2^-(k) = \min_{k_1, k_2=k-k_1} \left(\omega(k_1) + \omega(k_2) \right) . \quad (3)$$

Starting from the symmetric state $(k_1, k_2) = (k/2, k/2)$, with energy $\omega_2(k) = 2\omega(k/2)$, we can establish this lower boundary $\Omega_2^-(k)$ by shifting these momenta to $(k_1, k_2) = (k/2 - \Delta, k/2 + \Delta)$, and determining whether any nonzero, physically distinct Δ ($0 < \Delta \leq \pi$) gives a lower-energy two-magnon state. (See Fig.2 for this construction.) The condition that the initial, symmetric state itself has the lowest energy is

$$\omega(k/2 - \Delta) + \omega(k/2 + \Delta) - 2\omega(k/2) > 0 \quad \forall \Delta , \quad (4)$$

which can be used as the definition of a ‘‘globally concave’’ function. (A function is locally concave if this is satisfied for infinitesimal Δ .) The lower boundary curve of the two-magnon continuum is given by

$$\Omega_2^-(k) = 2\omega(k/2) \quad (5)$$

if the one-magnon dispersion is globally concave.

Both upper and lower boundaries will usually be extremal in the energy of two magnon states, so that they satisfy

$$d\omega_2(k_1, k - k_1) = 0 = \left(\omega'(k_1) - \omega'(k - k_1) \right) dk_1 \quad (6)$$

or equivalently

$$\omega'(k/2 - \Delta) = \omega'(k/2 + \Delta) . \quad (7)$$

The search for boundary curves of this extremal type can be considered a search for the minimum- or maximum-energy solutions $\Delta^\pm(k)$ of this equation; once (7) is solved for $\Delta^\pm(k)$, the boundary curves are then given by

$$\Omega_2^\pm(k) = \omega(k/2 - \Delta^\pm(k)) + \omega(k/2 + \Delta^\pm(k)) . \quad (8)$$

Clearly one solution of (7) is $\Delta(k) = 0$, giving $\Omega_2(k) = 2\omega(k/2)$. This may however not give the global minimum or maximum two-magnon energy at k . We shall argue below that the lower boundary is in fact *not* given by $\Delta(k) = 0$ if $\omega(k/2)$ is convex.

If the one-magnon dispersion relation $\omega(k)$ is not locally concave over the full physically independent range $[-\pi, \pi]$, the concave region $[-k_0, k_0]$ will be bounded by inflection points at $k = \pm k_0$. For a two-magnon state with momentum $|k| > 2k_0$ (which lies in the convex region of the one-magnon dispersion relation) the lower boundary of the two-magnon continuum is not given by $2\omega(k/2)$, since an infinitesimal perturbation into an unsymmetric state $(k_1, k_2) = (k/2 - \Delta, k/2 + \Delta)$ lowers the energy;

$$\lim_{\Delta \rightarrow 0} \omega(k/2 - \Delta) + \omega(k/2 + \Delta) - 2\omega(k/2) = \Delta^2 \omega''(k/2) + O(\Delta^4) < 0 . \quad (9)$$

The nature of the departure of $\Omega_2^-(k)$ from the symmetric state as we enter the convex region depends on the behavior of $\omega(k)$ near the inflection point k_0 . If the departure from the symmetric state $\Delta(k) = 0$ is continuous, $\Delta(k)$ will be small near $k = 2k_0$, and we can expand (7) to find

$$\lim_{k \rightarrow 2k_{0+}} \Delta(k) = \left[\frac{-6w^{(ii)}(k/2)}{w^{(iv)}(k/2)} \right]^{1/2} . \quad (10)$$

We can further simplify this by expanding in $k - 2k_0$ and using $\omega''(k_0) = 0$, which gives

$$\lim_{k \rightarrow 2k_{0+}} \Delta(k) = \left[\frac{-3w^{(iii)}(k_0)}{w^{(iv)}(k_0)} \right]^{1/2} (k - 2k_0)^{1/2}. \quad (11)$$

Thus if the fourth derivative $\omega^{(iv)}(k_0)$ is positive ($\omega^{(iii)}(k_0) < 0$ at this inflection point), the minimum energy state $(k_1, k_2) = (k/2 - \Delta(k), k/2 + \Delta(k))$ departs from the symmetric one $(k/2, k/2)$ as a square root of momentum.

The corresponding departure in energy of $\Omega_2^-(k)$ from $2\omega(k/2)$ is much less abrupt, and for small $k - 2k_0$ is

$$\lim_{k \rightarrow 2k_{0+}} \Omega_2^-(k) - 2\omega(k/2) = -\frac{3}{4} \left[\frac{w^{(iii)}(k_0)^2}{w^{(iv)}(k_0)} \right] (k - 2k_0)^2. \quad (12)$$

This piecewise continuous behavior and square-root departure in composition (k_1, k_2) from symmetric states on $\Omega_2^-(k)$ near $2k_0$ is illustrated by the alternating chain in Fig.3. In this model to leading order in α (see Appendix) one has $k_0 - \pi/2 = -\alpha/2$, $w^{(iii)}(k_0) = -\alpha/2$ and $w^{(iv)}(k_0) = 3\alpha^2/4$, so

$$\lim_{\substack{k \rightarrow 2k_{0+} \\ \alpha \rightarrow 0}} \Delta(k) = \left(\frac{2}{\alpha} \right)^{1/2} (k - (\pi - \alpha))^{1/2} \quad (13)$$

and

$$\lim_{\substack{k \rightarrow 2k_{0+} \\ \alpha \rightarrow 0}} \Omega_2^-(k) - 2\omega(k/2) = -\frac{1}{4} (k - (\pi - \alpha))^2. \quad (14)$$

The location of this composition discontinuity could be used as an independent experimental determination of α that does not require following $\omega(k)$ over a wide range of k .

Between $|k| = 2k_0$ and $|k| = \pi$ the two-magnon lower boundary passes through states of increasingly unsymmetrical composition, reaching the limit $k_1 = 0, |k_2| = \pi$ at $|k| = \pi$. This is illustrated in Fig.3.

Were $w^{(iv)}(k_0)$ negative we would find a discontinuous jump in the value of k_1 on the boundary $\Omega_2^-(k)$ at $k = 2k_0$. In either case we expect to see rapid variation in scattering intensities from states near this composition discontinuity.

1.3 Upper continuum boundary

The upper two-magnon continuum boundary, defined by

$$\Omega_2^+(k) = \max_{k_1, k_2=k-k_1} \left(\omega(k_1) + \omega(k_2) \right), \quad (15)$$

can be found using a similar construction to Fig.2. First note that the global maximum of energy of two-magnon states is $2\omega(\pi)$, at $k = 2\pi$ (equivalent to $k = 0$ or any $k = 2\pi m$) and consists of a symmetric state of two magnons, $k_1 = k_2 = \pi$. As we move away from this highest-energy state at $k = 2\pi$, we can form analogous symmetric states with total momentum $2\pi - k$ (equivalent to $-k$ and degenerate with a k state) from two single-magnon states with $k_1 = k_2 = \pi - k/2$, as shown in Fig.4. Evidently this state has energy $2\omega(\pi - k/2)$. We can determine whether this is the maximum energy state at this k by considering a symmetrically displaced combination $(k_1, k_2) = (\pi - k/2 - \Delta, \pi - k/2 + \Delta)$, analogous to Fig.2. The energy difference is

$$\Delta E = \omega(\pi - k/2 + \Delta) + \omega(\pi - k/2 - \Delta) - 2\omega(\pi - k/2), \quad (16)$$

which is negative for all k in $[0, \pi]$ (meaning that the symmetric state has the highest energy) if $\omega(k)$ is convex over the range $[\pi/2, \pi]$. If this is satisfied the upper boundary curve of the two-magnon continuum is given by

$$\Omega_2^+(k) = 2\omega(\pi - k/2) . \quad (17)$$

This is the case for our alternating chain example, as is shown in Fig.4. It is also satisfied for the uniform $S = 1/2$ Heisenberg chain, for which $\omega(k) = (\pi/2)J |\sin(k)|$; since this is a convex function, (17) implies

$$\Omega_2^+(k) = 2\omega(\pi - k/2) = \pi J |\sin(k/2)| , \quad (18)$$

which is the well-known upper boundary of the two-spinon continuum [8].

If instead we encounter an inflection point $\omega''(k_0) = 0$ in the interval $[\pi/2, \pi]$, we will find a departure from $2\omega(\pi - k/2)$ along the upper boundary. As in Fig.3 this will be accompanied by a change in composition from the symmetric state $(k_1, k_2) = (\pi - k/2, \pi - k/2)$.

Since we have assumed for our example that the inflection point k_0 lies in the interval $[0, \pi/2]$, we do not encounter an inflection point, and the function $\Omega_2^+(k) = 2\omega(\pi - k/2)$ describes the entire upper boundary curve for $k \in [-\pi, \pi]$. This function is monotonically decreasing inside the range $k = [0, \pi]$, and has a negative slope at $k = \pi$, given our assumption that $\omega(k)$ has a positive slope at $\pi/2$. Reflection symmetry of the dispersion relation about $k = \pi$ then implies a cusp in the slope of the upper boundary curve at $k = \pi$, as shown in Fig.4.

In Fig.5 we show the complete result for the boundary curves $\Omega_2^+(k)$ and $\Omega_2^-(k)$ of the two-magnon continuum for our alternating chain example. Note that the two-magnon bandwidth minimum at $k = \pi$ is not zero; the value

$$W_2^{min} = \Omega_2^+(\pi) - \Omega_2^-(\pi) = 2\omega(\pi/2) - \omega(0) - \omega(\pi) , \quad (19)$$

is $\alpha^2/4 + \alpha^3/8 + O(\alpha^4)$ for the alternating chain. A zero bandwidth at $k = \pi$ would follow for example from pure $\cos(k)$ modulation in the one-magnon dispersion relation.

1.4 More general boundary curves

Motivated by the alternating chain as a prototypical gapped 1D quantum spin system, we have assumed that the one-magnon dispersion relation is even, monotonically increasing inside $[0, \pi]$, and has a single inflection point at k_0 inside $[0, \pi/2]$. This led to an upper two-magnon continuum boundary with a cusp and a symmetric composition $k_1 = k_2$ everywhere, and a lower two-magnon boundary with a composition break at $2k_0$.

Although these results are valid in general for alternating chains, in other quantum spin systems we may encounter a single inflection point in $[\pi/2, \pi]$, or a different number of inflection points. An example of more complicated behavior is provided by the two-leg ladder, which for sufficiently large α has a one-magnon dispersion relation $\omega(k)$ with a minimum at $k = \pi$, a secondary minimum at $k = 0$, two inflection points in $k \in [0, \pi]$, and a maximum at an intermediate $k \in [0, \pi/2]$.

We expect to find a symmetric state $k_1 = k_2 = k/2$ at the lower boundary $\Omega_2^-(k)$ of the continuum when $\omega(k/2)$ is globally concave, and an unsymmetric two-magnon state on $\Omega_2^-(k)$ with an energy $< 2\omega(k/2)$ when $\omega(k/2)$ is a locally or globally convex function of k . With more than one inflection point, boundary curves will typically be composed of pieces with symmetric and asymmetric composition.

1.5 Density of states: caustics

Our results for the composition of two-magnon states along the upper and lower continuum boundaries imply the existence of discontinuities in the density of states on the continuum boundary and under certain conditions within the continuum. We refer to any such discontinuity in the density of states as a “caustic”.

Consider the density of states in a system of N spins with unit cell b ; the number of one-magnon states dn in an interval dk is

$$dn = \left(\frac{2\pi}{Nb} \right) dk \equiv n_0 dk . \quad (20)$$

and for two-magnon states in $dk_1 dk_2$ it is

$$d^2n = n_0^2 dk_1 dk_2 . \quad (21)$$

Since we observe two-magnon continuum states with specified total energy $E = \omega(k_1) + \omega(k_2) + E_0$ and total momentum $k = k_1 + k_2$, the number of states d^2n in a region $dk dE$ is more relevant to experiment. This density has a Jacobean factor,

$$d^2n = \frac{n_0^2}{|\omega'(k_1) - \omega'(k_2)|} dk dE \equiv \rho(k, E) dk dE . \quad (22)$$

Note that the condition for a divergent density of states $\rho(k, E)$, which is a singular caustic, is

$$\omega'(k_1) = \omega'(k_2) , \quad (23)$$

which was exactly the condition (7) used to search for boundaries of the two-magnon continuum. Thus we expect to find a divergent density of states $\rho(k, E)$ on the two-magnon boundary curves $\Omega_2^-(k)$ and $\Omega_2^+(k)$.

Unfortunately we cannot invert the $(E, k) \leftrightarrow (k_1, k_2)$ relationship and solve (22) for $\rho(k, E)$ for a general one-magnon dispersion relation $\omega(k)$. We can however determine this density of two-magnon states in certain limits, including the case of states close to the boundaries.

First we consider the symmetric lower boundary $\Omega_2^-(k) = 2\omega(k/2)$. (Recall that $2\omega(k/2)$ gives the lower boundary of the two-magnon continuum for a range of k , as discussed in previous sections.) Perturbing the momenta away from this symmetric point into the continuum of asymmetric states, we can invert $(E, k) \leftrightarrow (k_1, k_2)$ infinitesimally and use (22) to find the density of states $\rho(k, E)$ near $2\omega(k/2)$. This gives

$$\lim_{E \rightarrow 2\omega(k/2)} \rho(k, E) = \frac{n_0^2}{2 |\omega''(k/2)|^{1/2}} \left| E - 2\omega(k/2) \right|^{-1/2} . \quad (24)$$

which evidently has a $1/\sqrt{\Delta E}$ singularity as we approach $2\omega(k/2)$. This behavior is reminiscent of the van Hove singularity in the density of states as we approach a band edge, although that single particle density is instead proportional to $1/|\omega'(k)|$.

The asymmetric region of $\Omega_2^-(k)$ with $k_1 < k_2$ also has a singular density of states, since $\omega'(k_1) = \omega'(k_2)$ there as well. We may again solve for $\rho(k, E)$ near the boundary using (22), with the result

$$\lim_{E \rightarrow \omega(k_1) + \omega(k_2)} \rho(k, E) = \frac{n_0^2}{2 (\omega''(k_1) + \omega''(k_2))^{1/2}} \left| E - \omega(k_1) - \omega(k_2) \right|^{-1/2} \quad (25)$$

where $(k_1, k_2) = k/2 \mp \Delta(k)$. The symmetric boundary formula (24) is a special case of this more general result.

A final special case is the density of states in E along the line $k = 2k_0$; since $\omega''(k_0) = 0$ this is a singular case. Expanding (7) to $O(\Delta^3)$ (the usual leading $O(\Delta)$ term vanishes), we find

$$\lim_{E \rightarrow 2\omega(k_0)} \rho(k = 2k_0, E) = n_0^2 \left[\frac{3}{4 |\omega^{(iv)}(k_0)|} \right]^{1/4} |E - 2\omega(k_0)|^{-3/4}. \quad (26)$$

Although we have specifically discussed the singular density of states found at the upper and lower boundaries $\Omega_2^\pm(k)$, we note that there may be caustics specified by (7) *within* the continuum as well, and that these will also have square-root divergences in $\rho(k, E)$ as we approach the singular line.

We again use the alternating chain to illustrate this. In Fig.6 we show points in the two-magnon continuum, generated with a $\rho(k, E)$ distribution. The divergences in $\rho(k, E)$ on the upper and lower boundaries, “border caustics”, are evident (see also Fig.10). Fig.7 shows an enlargement including the asymmetric region $k > 2k_0$; a caustic *within* the continuum due to the solution $\omega_2(k) = 2\omega(k/2)$ of (7) is apparent.

1.6 Spin ladder

As an independent example of a two-magnon continuum, in Fig.8 we show the one-magnon dispersion $\omega(k)$ and two-magnon continuum for a two-leg spin ladder, as in Fig.6 for the alternating chain. The coupling strengths are $\alpha \equiv J_{||}/J_{\perp} = 0.3$ and $J_{\perp} = 1$, and the analytic results used are summarized in the appendix.

Although the ladder one-magnon $\omega(k)$ has the locations of maxima and minima translated by π relative to the alternating chain, the two-magnon continua of the two systems are qualitatively remarkably similar for small α . This is because a shift in k by 2π , for two magnons, is equivalent to zero. Close inspection reveals that the α -dependent effects are typically rather larger on the ladder than the alternating chain, presumably because the ladder dimers are coupled by twice as many links as the alternating-chain dimers.

2 Higher multimagnon states

2.1 Definitions

Higher multimagnon continua show features similar to the cusps and discontinuities of two-magnon states, although these will presumably be of much less experimental interest due to the weaker coupling of higher-lying states to experimental probes. We shall nonetheless sketch the generalization of some of the simpler results for two-magnon systems to the n -magnon continua.

The energy of an n -magnon state is given by

$$\omega_n(k) = \sum_{m=1}^n \omega(k_m) \quad (27)$$

where

$$k = \sum_{m=1}^n k_m \text{ mod } (2\pi). \quad (28)$$

Again assuming a gapped one-magnon dispersion relation with the general features discussed in the previous section (an even $\omega(k)$, monotonically increasing inside $[0, \pi]$, quadratic behavior in k near these endpoints, and a single inflection point k_0), we can infer several features of the n -magnon continuum.

2.2 N-magnon continuum boundaries

Provided that the individual magnon momenta k/n are below the inflection point k_0 , ($k < nk_0 \forall k \in [0, \pi]$), the lower boundary $\Omega_n^-(k)$ of the n -magnon continuum is given by the energy of the symmetric state $(k_1, k_2 \dots k_n) = (k/n, k/n \dots k/n)$,

$$\Omega_n^-(k) = n\omega(k/n) \quad (29)$$

This implies that for sufficiently large n ($n > \pi/k_0$) all the lower-boundary curves $\{\Omega_n^-(k)\}$ possess cusps at $k = \pi$. Since the departure of $\omega(k)$ from $\omega(0)$ for small k is assumed to be of the form $\omega(k) = \omega(0) + c_2 k^2 + O(k^4)$, the lower boundary curve will approach

$$\lim_{n \rightarrow \infty} \Omega_n^-(k) = n\omega(0) + (c_2/n)k^2 + O(n^{-3}) . \quad (30)$$

Thus $\Omega_n^-(k)$ asymptotically approaches the line $n\omega(0)$, with a residual $O(n^{-1})$ parabolic component $\propto k^2/n$.

The upper boundary $\Omega_n^+(k)$ differs for even and odd magnon number. For an even number of magnons the upper boundary maximum energy $n\omega(\pi)$ occurs at $k = n\pi \equiv 0$. Again assuming quadratic behavior near the extremum, $\omega(k) = \omega(\pi) - \tilde{c}_2(\pi - k)^2 + O((\pi - k)^4)$, the symmetric solution $(k_1, k_2 \dots k_n) = (\pi - k/n, \pi - k/n \dots \pi - k/n)$ with energy

$$\Omega_n^+(k) = n\omega(\pi - k/n) \quad (31)$$

gives the upper boundary curve provided that we do not encounter an inflection point, $\pi - k/n > k_0$. Once again this will be satisfied for sufficiently large n , and all these even- n upper boundary curves have a cusp at $k = \pi$. The behavior of this upper boundary for large n approaches a constant with a negative parabolic component of $O(n^{-1})$,

$$\Omega_n^+(k) = n\omega(\pi) - (\tilde{c}_2/n)k^2 + O(n^{-3}) , \quad (32)$$

analogous to the result for the lower boundary. The upper boundary for odd magnon number n differs in that the maximum energy state has total momentum $k = \pi$ rather than $k = 0$, and a cusp at $k = 0$ rather than $k = \pi$.

2.3 Caustics

The higher multimagnon continua also possess discontinuities in their densities of states $\{\rho(k, E)\}$, although these are qualitatively different from the results we have shown for the two-magnon case. This is largely due to the fact that the $(k_1, k_2) \rightarrow (k, E)$ mapping gives a simple Jacobean (22) which leads to caustics where it is singular, whereas the $n \geq 3$ multimagnon continua project a flat distribution in $(k_1, k_2, \dots k_n)$ onto a smaller number of variables (k, E) . This involves an integration over $n - 2$ variables, which smoothes the singularities seen in the two-magnon case.

As examples of these higher continua, in Fig.9 we show the three-magnon continuum for our alternating chain example, and Fig.10 shows the density of states encountered in a fixed- k slice (at $k = \pi/2$) through the two-, three-, and four-magnon continua. (This figure is a histogram of points falling within $0.495\pi < k < 0.505\pi$, with an energy binning of $\delta E = 0.01$, normalized as $f(k, E) = N(k, E)/\delta E \delta k N_{tot.}$. The binned points were selected from an initial flat distribution, $-\pi < k_1, k_2 \dots k_n < \pi$, of $N_{tot.} = 2^{28}$ points.)

The two-magnon continuum in Figs.9,10 clearly shows the $1/\sqrt{\Delta E}$ singular border caustics in the density of states, as given by (24). In contrast, the three-magnon continuum density $\rho(k, E)$ has border caustics with only finite discontinuities in the density of states, and the four-magnon $\rho(k, E)$ is continuous on the boundaries.

3 Summary and Conclusions

We have considered the multimagnon continua of 1D quantum spin systems, and have illustrated our results using the Heisenberg alternating chain and two-leg spin ladder as examples.

The boundaries of the two-magnon continua that result from one-magnon dispersion relations similar to the alternating chain case are considered in detail, and general results are derived for these and higher multimagnon boundary curves. It is shown that these curves exhibit cusps and discontinuous changes in composition under certain conditions. The density of states $\rho(k, E)$ in the continuum is also considered, and it is noted that $\rho(k, E)$ can possess discontinuities and divergences on “caustic” lines, both on the continuum boundaries and within the continuum.

We anticipate that it should be possible to identify these features of two-magnon continua through high-resolution inelastic neutron scattering experiments on candidate alternating chain and ladder materials, and that precise studies of these features may allow determinations of the parameters of spin Hamiltonians through the study of relatively small ranges of (k, E) space.

4 Acknowledgements

It is a pleasure to thank B. Lake, G.I. Meijer, G. Müller, S.E. Nagler, T. Papenbrock, J. Riera, R.R.P. Singh, D.A. Tennant and G.S. Uhrig for useful discussions and communications. This research was sponsored by the Laboratory Directed Research and Development Program of Oak Ridge National Laboratory (ORNL), managed by UT-Battelle, LLC for the U.S. Department of Energy under Contract No. DE-AC05-00OR22725, and by the Department of Physics and Astronomy, the Neutron Sciences Consortium, and the Chemical Physics Program of the University of Tennessee.

Appendix: results for alternating chains and ladders

In this appendix we collect some results for the alternating Heisenberg chain and two-leg ladder, which we used to illustrate aspects of multimagnon continuum states in the paper.

The alternating chain Hamiltonian is defined by

$$H = J \sum_{i=1}^{N/2} \vec{S}_{2i-1} \cdot \vec{S}_{2i} + \alpha \vec{S}_{2i} \cdot \vec{S}_{2i+1} , \quad (\text{A1})$$

where we assume cyclic boundary conditions. The corresponding one-magnon dispersion relation $\omega(k)$ can be written as a Fourier series, with α -dependent coefficients;

$$\omega(k) = \sum_{\ell=0}^{\infty} a_{\ell}(\alpha) \cos(\ell k) , \quad (\text{A2})$$

where we have implicitly set the strength J and unit cell b to unity. The Fourier coefficients may be evaluated as a power series in α using a strong-coupling expansion. The $O(\alpha^5)$ series of Ref.[9], which we use to generate the numerical results given in this paper, are

$$\begin{aligned} a_0 &= 1 & -\frac{1}{16} \alpha^2 & +\frac{3}{64} \alpha^3 & +\frac{23}{1024} \alpha^4 & -\frac{3}{256} \alpha^5 \\ a_1 &= & -\frac{1}{2} \alpha & -\frac{1}{4} \alpha^2 & +\frac{1}{32} \alpha^3 & +\frac{5}{256} \alpha^4 & -\frac{35}{2048} \alpha^5 \\ a_2 &= & & -\frac{1}{16} \alpha^2 & -\frac{1}{32} \alpha^3 & -\frac{15}{512} \alpha^4 & -\frac{283}{18432} \alpha^5 \\ a_3 &= & & & -\frac{1}{64} \alpha^3 & -\frac{1}{48} \alpha^4 & -\frac{9}{1024} \alpha^5 \\ a_4 &= & & & & -\frac{5}{1024} \alpha^4 & -\frac{67}{9216} \alpha^5 \\ a_5 &= & & & & & -\frac{7}{4096} \alpha^5 \end{aligned} . \quad (\text{A3})$$

We may use these coefficients to develop series for several of the quantities discussed here. In particular, the inflection point k_0 of $\omega(k)$ is given by

$$k_0 = \frac{\pi}{2} - \frac{1}{2} \alpha - \frac{29}{96} \alpha^3 - \frac{119}{576} \alpha^4 + O(\alpha^5) \quad (\text{A4})$$

and the energy $\Omega_2^-(2k_0)$ at the ‘‘break point’’ $2k_0$ (see Fig.3) on the lower boundary of the two-magnon continuum is given by

$$\Omega_2^-(2k_0) = 2\omega(k_0) = 2 - \frac{1}{2} \alpha^2 - \frac{3}{32} \alpha^3 - \frac{11}{64} \alpha^4 - \frac{311}{1024} \alpha^5 + O(\alpha^6) . \quad (\text{A5})$$

The derivatives of the one-magnon energy $\omega(k)$ at k_0 determine the nature of the asymmetric two-

magnon lower boundary state for $k > 2k_0$. To $O(\alpha^5)$ these are

$$\begin{aligned}
\omega'(k_0) &= +\frac{1}{2}\alpha + \frac{1}{4}\alpha^2 - \frac{1}{64}\alpha^3 - \frac{13}{256}\alpha^4 + \frac{229}{4096}\alpha^5 \\
\omega''(k_0) &= 0 \\
\omega^{(iii)}(k_0) &= -\frac{1}{2}\alpha - \frac{1}{4}\alpha^2 + \frac{1}{64}\alpha^3 + \frac{93}{256}\alpha^4 - \frac{925}{4096}\alpha^5 \\
\omega^{(iv)}(k_0) &= +\frac{3}{4}\alpha^2 + \frac{3}{8}\alpha^3 + \frac{63}{128}\alpha^4 + \frac{257}{512}\alpha^5
\end{aligned} \tag{A6}$$

We also give the corresponding results for the two-leg spin ladder (to one higher order in α). The N -rung ladder Hamiltonian is given by

$$H = J_{\perp} \sum_{i=1}^N \vec{S}_{i,1} \cdot \vec{S}_{i,2} + \alpha (\vec{S}_{i,1} \cdot \vec{S}_{i+1,1} + \vec{S}_{i,2} \cdot \vec{S}_{i+1,2}), \tag{A7}$$

and the $\omega(k)$ one-magnon Fourier coefficients to $O(\alpha^6)$ are:

$$\begin{aligned}
a_0 &= 1 + \frac{3}{4}\alpha^2 + \frac{3}{8}\alpha^3 - \frac{13}{64}\alpha^4 - \frac{5}{8}\alpha^5 - \frac{1}{2}\alpha^6 \\
a_1 &= +\alpha - \frac{1}{4}\alpha^3 - \frac{5}{16}\alpha^4 - \frac{13}{64}\alpha^5 + \frac{3}{32}\alpha^6 \\
a_2 &= -\frac{1}{4}\alpha^2 - \frac{1}{4}\alpha^3 - \frac{1}{32}\alpha^4 + \frac{13}{64}\alpha^5 + \frac{11}{64}\alpha^6 \\
a_3 &= +\frac{1}{8}\alpha^3 + \frac{1}{8}\alpha^4 - \frac{3}{32}\alpha^5 - \frac{81}{256}\alpha^6 \\
a_4 &= -\frac{5}{64}\alpha^4 - \frac{3}{32}\alpha^5 + \frac{73}{1024}\alpha^6 \\
a_5 &= +\frac{7}{128}\alpha^5 + \frac{5}{64}\alpha^6 \\
a_6 &= -\frac{21}{512}\alpha^6
\end{aligned} \tag{A8}$$

The inflection point k_0 is:

$$k_0 = \frac{\pi}{2} + \alpha + \alpha^2 + \frac{2}{3}\alpha^3 - \frac{1}{2}\alpha^4 - \frac{1171}{320}\alpha^5 + O(\alpha^6) \tag{A9}$$

and the lower boundary energy $\Omega_2^-(2k_0)$ at the break point $2k_0$ is:

$$\Omega_2^-(2k_0) = 2\omega(k_0) = 2 - \frac{3}{4}\alpha^3 - \frac{5}{4}\alpha^4 - \frac{7}{32}\alpha^5 + \frac{3307}{512}\alpha^6 + O(\alpha^7). \tag{A10}$$

Finally, the derivatives of $\omega(k)$ at k_0 are:

$$\begin{aligned}
 \omega'(k_0) &= -\alpha && +\frac{1}{8}\alpha^3 && -\frac{5}{16}\alpha^4 && -\frac{117}{128}\alpha^5 && -\frac{223}{256}\alpha^6 \\
 \omega''(k_0) &= 0 \\
 \omega^{(iii)}(k_0) &= +\alpha && -\frac{1}{8}\alpha^3 && +\frac{53}{16}\alpha^4 && +\frac{1005}{128}\alpha^5 && +\frac{1927}{256}\alpha^6 \\
 \omega^{(iv)}(k_0) &= && +3\alpha^2 && +3\alpha^3 && +\frac{21}{8}\alpha^4 && +\frac{177}{16}\alpha^5 && +\frac{1557}{128}\alpha^6
 \end{aligned} \tag{A11}$$

References

- [1] See for example B.S.Shastry and B.Sutherland, Phys. Rev. Lett. 47, 964 (1981); G.S.Uhrig and H.J.Schulz, Phys. Rev. B54, R9624 (1996); *ibid.*, Phys. Rev. B58, 2900 (1998); K.Damle and S.Sachdev, cond-mat/9711014, Phys. Rev. B57, 8307 (1998); O.P.Sushkov and V.N.Kotov, Phys. Rev. Lett. 81, 1941 (1998); V.N.Kotov, O.P.Sushkov and R.Eder, Phys. Rev. B59, 6266 (1999); R.R.P.Singh and Z.Weihong, cond-mat/9811028, Phys. Rev. B59, 9911 (1999); K.Damle and S.E.Nagler, cond-mat/9904438; C.Jurecka and W.Brenig, Phys. Rev. B61, 14307 (2000); S.Trebst, H.Monien, C.J.Hamer, Z.Weihong and R.R.P.Singh, cond-mat/0007192, Phys. Rev. Lett. 85, 4373 (2000); W.Zheng, C.J.Hamer, R.R.P.Singh, S.Trebst and H.Monien, cond-mat/0010354, Phys. Rev. B63, 144410 (2001); W.Zheng, C.J.Hamer, R.R.P.Singh, S.Trebst and H.Monien, cond-mat/0010243, Phys. Rev. B 63, 144411 (2001).
- [2] D.A.Tennant, C.Broholm, D.H.Reich, S.E.Nagler, G.E.Granroth, T.Barnes, G.Xu, B.C.Sales and Y.Chen, cond-mat/0005222.
- [3] M.Windt, M.Grüninger, T.Nunner, C.Knetter, K.Schmidt, G.S.Uhrig, T.Kopp, A.Freimuth, U.Ammerahl, B.Büchner and A.Revcolevschi, cond-mat/0103438.
- [4] M.Grüninger, M.Windt, T.Nunner, C.Knetter, K.P.Schmidt, G.S.Uhrig, T.Kopp, A.Freimuth, U.Ammerahl, B.Büchner and A.Revcolevschi, cond-mat/0109524.
- [5] G.I.Meijer, *Magnetic Correlations in the One-Dimensional Quantum Magnets $Sr_{0.73}CuO_2$ and $Ca_{0.73}CuO_2$ and the Mott-Hubbard System $LaTiO_3$* , ETH PhD dissertation No.13128.
- [6] J.H.Taylor and G.Müller, Physica 130A, 1 (1985). This reference discusses the two-particle continuum of an alternating 1D XY model, which leads to results very similar to the alternating Heisenberg chain and two-leg ladder examples we consider.
- [7] M.Karbach and G.Müller, Phys. Rev.B62, 14871 (2000). This reference studies magnetic field effects on continuum states of the uniform 1D Heisenberg chain.
- [8] J. Des Cloizeaux and J.J.Pearson, Phys. Rev. 128, 2131 (1962).
- [9] T.Barnes, J.Riera and D.A.Tennant, Phys. Rev. B59, 11384 (1999).

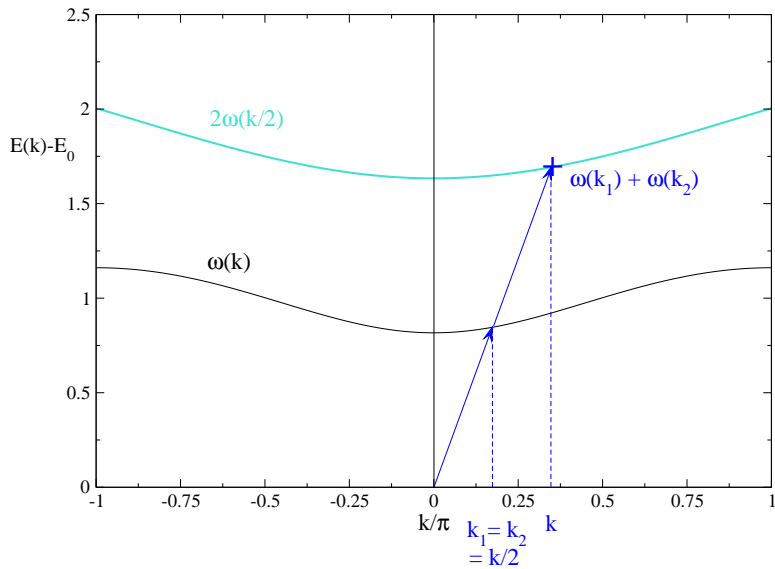


Figure 1. The alternating chain one-magnon dispersion relation $\omega(k)$ for $J = 1$ and $\alpha = 0.3$, showing a symmetric two-magnon state.

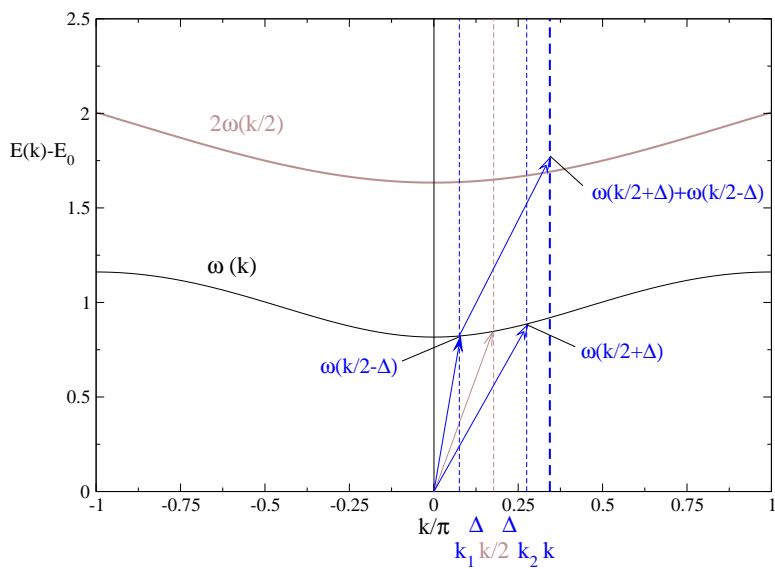


Figure 2. Illustrating the construction of an asymmetric two-magnon state (4).

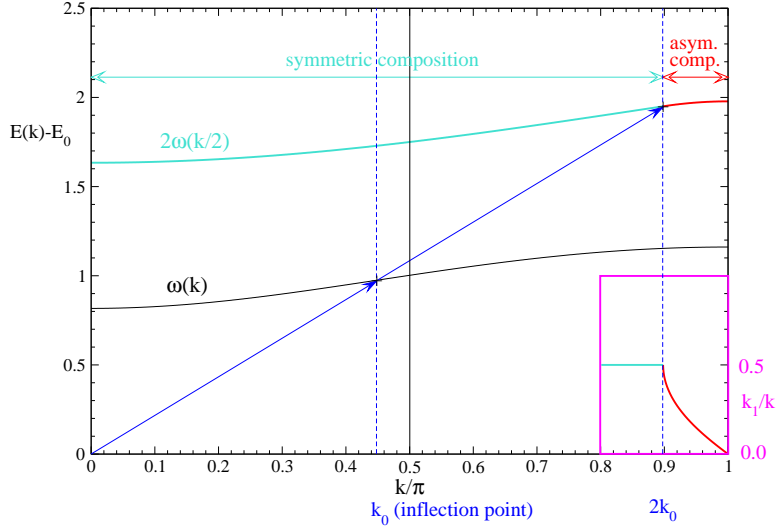


Figure 3. The $k = 2k_0$ transition from symmetric ($k_1 = k_2$) to asymmetric ($k_1 < k_2$) states on the lower boundary $\Omega_2^-(k)$ of the two-magnon continuum. (Alternating chain, $J = 1$ and $\alpha = 0.3$; $2k_0/\pi = 0.898$, $\Omega_2^-(2k_0) = 1.950$.) The composition break in $k_1/(k_1 + k_2)$ is shown at lower right.

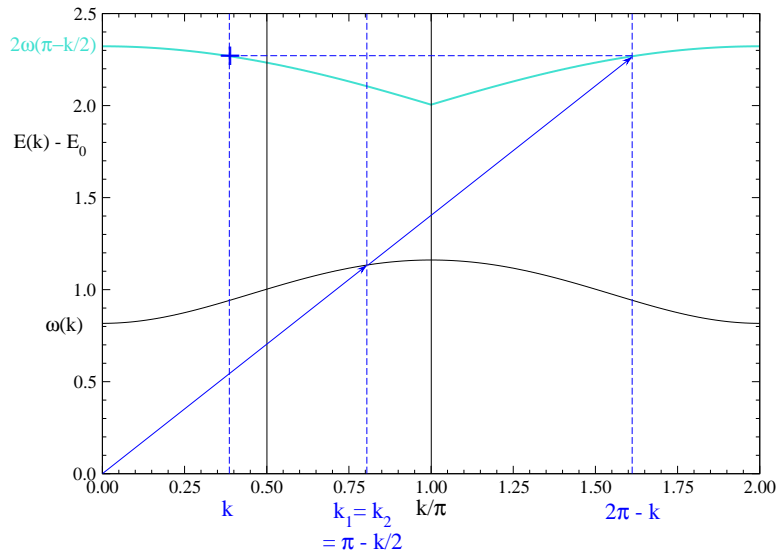


Figure 4. Construction of the two-magnon upper boundary $\Omega_2^+(k)$. (Alternating chain, $J = 1$ and $\alpha = 0.3$.)

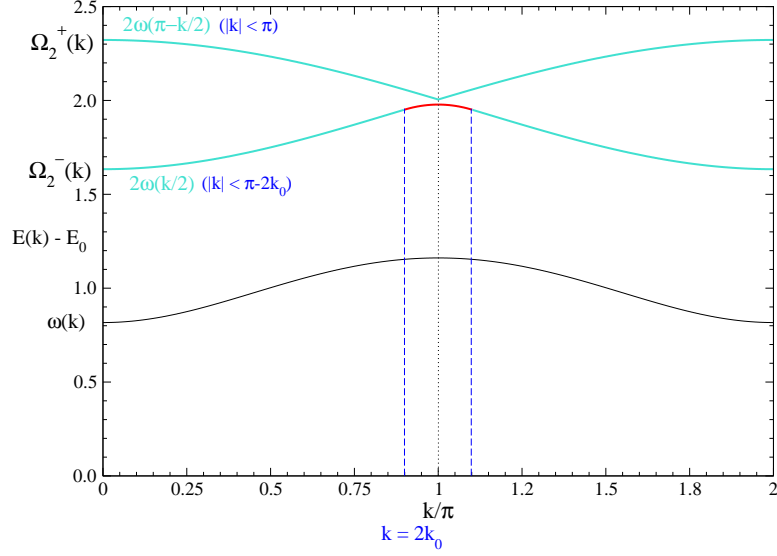


Figure 5. The complete two-magnon continuum boundary $\Omega_2^+(k)$ and $\Omega_2^-(k)$, showing the composition break at $k = 2k_0$. (Alternating chain, $J = 1$ and $\alpha = 0.3$.)

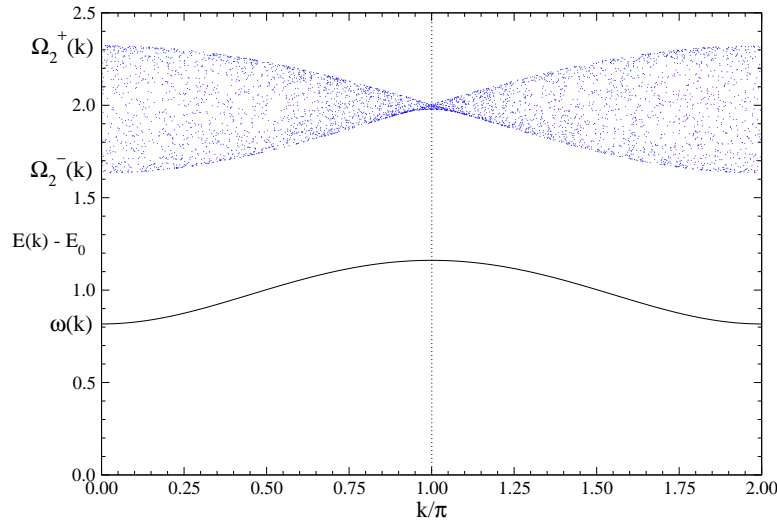


Figure 6. The density of two-magnon states within the continuum. (Alternating chain, $J = 1$ and $\alpha = 0.3$; flat distribution in k_1 and k_2 of 2^{12} states.)

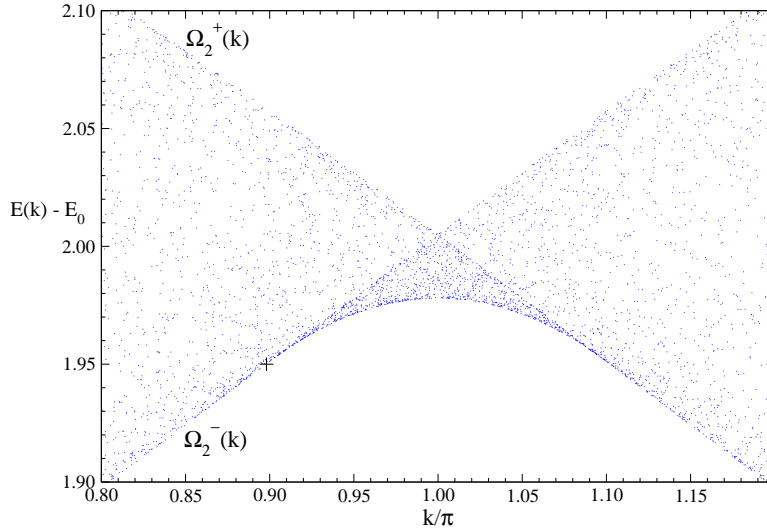


Figure 7. An enlargement of the alternating chain continuum of Fig.6, showing a discontinuity in the density of states $\rho(k, E)$ (a “caustic”) within the two-magnon continuum. The caustic is the line $2\omega(k/2)$ and its reflection about $k = \pi$. The composition break at $k = 2k_0$ where this curve departs from the lower continuum boundary $\Omega_2^-(k)$ is also indicated. (Flat distribution in k_1 and k_2 of 2^{12} states in the region displayed.)

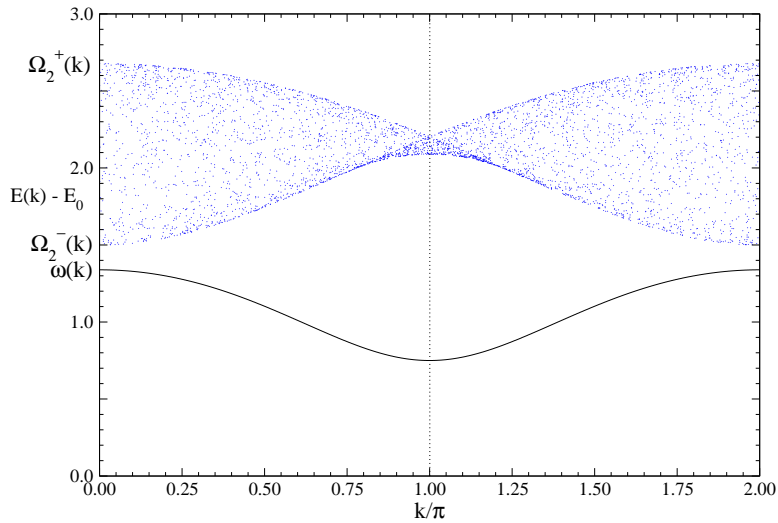


Figure 8. The one-magnon $\omega(k)$ and density of states within the two-magnon continuum for a two-leg spin ladder. ($J_{\perp} = 1$ and $\alpha = 0.3$; flat distribution in k_1 and k_2 of 2^{12} states.)

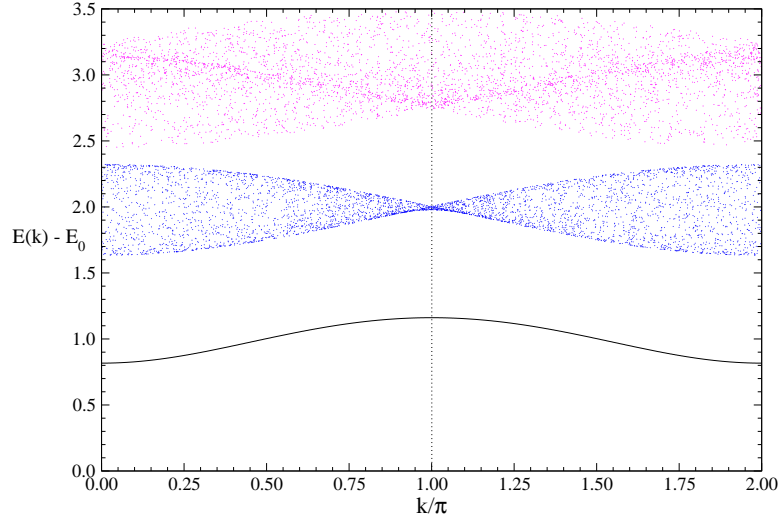


Figure 9. Two- and three-magnon continua of the alternating chain. ($J = 1$ and $\alpha = 0.3$; flat distribution in k_1 and k_2 of 2^{12} states in each case.)

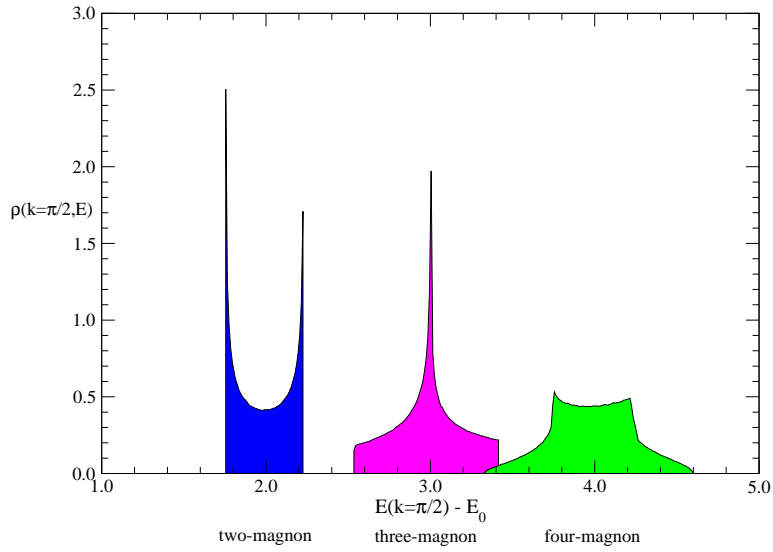


Figure 10. The density of states $\rho(k, E)$ encountered in a fixed- k slice ($k = \pi/2$) through the two-, three- and four-magnon continua. (Alternating chain, $J = 1$ and $\alpha = 0.3$.)